Robot Control for Rehabilitation: PD vs. LQG

Simona-Daiana Stiole
Department of Automation
Technical University of Cluj-Napoca
Cluj-Napoca, Romania
simona.sim@aut.utcluj.ro

Zsófia Lendek
Department of Automation
Technical University of Cluj-Napoca
Cluj-Napoca, Romania
zsofia.lendek@aut.utcluj.ro

Mircea Susca
Department of Automation
Technical University of Cluj-Napoca
Cluj-Napoca, Romania
mircea.susca@aut.utcluj.ro

Vlad-Mihai Mihaly
Department of Automation
Technical University of Cluj-Napoca
Cluj-Napoca, Romania
vlad.mihaly@aut.utcluj.ro

Petru Dobra
Department of Automation
Technical University of Cluj-Napoca
Cluj-Napoca, Romania
petru.dobra@aut.utcluj.ro

Paul Tucan
CESTER
Technical University of Cluj-Napoca
Cluj-Napoca, Romania
paul.tucan@mep.utcluj.ro

***Abstract*—This paper investigates and compares two control strategies for a DC motor actuating a joint of a rehabilitation robot intended for upper-limb recovery. A classical PD controller and a model-based LQG approach, are designed based on identified dynamics. Both controllers are first evaluated in simulation and are then tested on the physical motor using identical reference trajectories. Performance is assessed in terms of tracking accuracy, steady-state error, and sensitivity to measurement noise and modelling errors. The results highlight the practical trade-offs between the simplicity and tuning effort of the PD controller and the improved estimation and optimal feedback properties of the LQG scheme.**

***Keywords*—Rehabilitation Robotics; Motion Control; System Identification; LQG Control; Kalman Filter; Real-Time Implementation**

I. Introduction

DC motors remain a fundamental actuation solution in embedded control systems and robotic applications [1] due to their simplicity, efficiency, and low cost [2]. Accurate modeling and control of such actuators are essential for achieving stable and high-performance motion control. In practice, however, the available sensing is often limited, specifically, angular velocity is not directly measured [3], [4]. Instead, only position information is available through incremental encoders, and the velocity must be estimated [5].

Furthermore, when the system parameters are unknown, system identification [6], [7] provides an effective framework for deriving mathematical models directly from experimental data and have been widely applied to DC motor modeling [8]. Higher-order models improve accuracy, but for real-time applications, low-order discrete-time models are often preferred [9].

Optimal control strategies such as Linear Quadratic Regulation (LQR) [10] have been studied for motor control [11]. When combined with state estimation techniques, such as the Kalman filter, they form the Linear Quadratic Gaussian (LQG) framework. LQG control enables optimal feedback based on estimated states, but its practical implementation is often limited by modeling assumptions and sensor availability. Most existing studies [5], [12], [13] focus either on offline identification or on control design under ideal measurement conditions. Fewer works [14] address the complete pipeline with explicit consideration of real-time implementation.

Medical rehabilitation robots [15] are essential tools for delivering high-intensity, repetitive physical therapy and their movement is performed using DC motors. To address the control challenges of a multi-degree-of-freedom rehabilitation platform, this study adopts a decoupled approach by focusing on the identification and control of a single representative joint. Validating the identification procedure and the observer-based control architecture on this individual joint provides the experimental foundation for extension to the entire robotic system [16].

This paper proposes a complete identification and control framework for real-time embedded systems. A discrete-time model relating PWM input to motor velocity is identified from experimental data, resulting in a compact second-order state-space representation. A PD and an LQG control architecture are designed for the identified model. The controllers are validated using experimental data, and all parameters required for embedded implementation are provided.

The paper is structured as follows: Section II presents the rehabilitation robot, focusing on the specific joint and DC motor assembly. Section III details the identification of motor dynamics. Section IV describes the design of the classical PD controller and the LQG. Section V provides a comparative analysis of the results obtained from both simulations and real-time experiments. Finally, Section VI concludes this study.

II. Robot Description

The experimental platform used in this study is the WRIST-X rehabilitation robot [17] designed for upper-limb and wrist recovery, presented in Figure 1. The robot is intended to assist repetitive therapeutic movements under different rehabilitation strategies. It consists of multiple actuated joints, each driven by an electric motor and having position sensing.

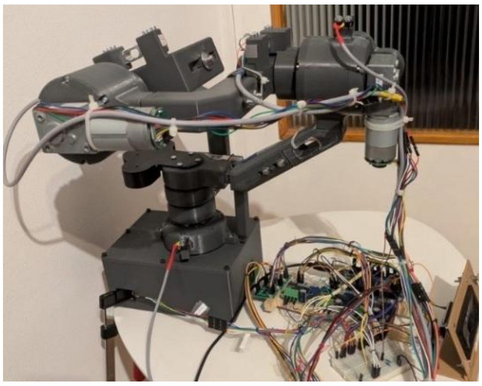

Fig. 1. Robot WRIST-X

Each joint of the robot is actuated by a DC motor and is associated with one fundamental wrist motion. Incremental encoders are used to measure joint position. No direct velocity or torque sensors are available

From a control perspective, the robot is modeled using an independent joint control approach. This assumption is valid for low-speed rehabilitation motions, where dynamic couplings between joints are limited and can be neglected or treated as disturbances for control. The control input for each joint is the pulse-width modulation (PWM) signal applied to the DC motor driver. The measured output is the joint position obtained from the encoder. A complete kinematic and dynamic model of the robot was derived in our previous work [17] using the Euler–Lagrange formulation, but motor dynamics and friction effects were neglected in order to focus on the mechanical behavior of the robot.

In the present study, control design is carried out at the joint level, based on experimentally identified dynamics, with the goal of implementing and validating control strategies in real time under realistic sensing and actuation constraints.

III. Identification of the 3rd Robot Joint

The joint is actuated by a DC motor. While the model of the DC motor, see [18], theoretically involves three state variables representing current, angular velocity, and angular position, experimental tests demonstrated [19] that the system dynamics can be effectively approximated using a reduced-order model by neglecting the current dynamics. Consequently, this study focuses on the identification of a model comprising only the velocity and position.

The identification was conducted using experimental data acquired at a sampling period of 0.01 seconds. The input signal consisted of the PWM duty cycle, while the measured output was the joint position provided by the encoder. To capture the dominant dynamics of the motor, a first-order model was identified to correlate the PWM input with the angular velocity reconstructed through numerical differentiation and filtered using a Butterworth filter. These signals can be seen in Figure 2.

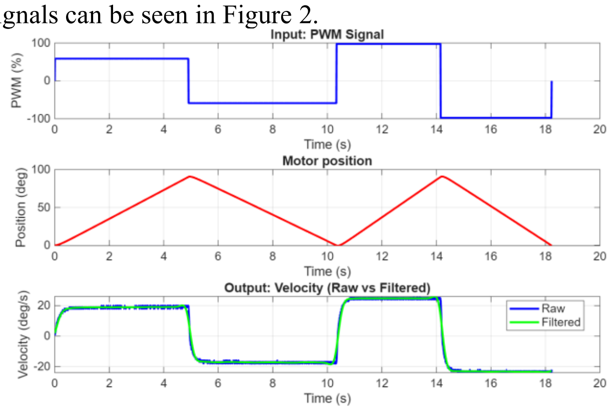

Fig. 2. Input and motor position

Various structures, namely n4sid, ARMAX, and OE have been tested. Among these, an ARX [1 1 0] model [20] provided the highest accuracy, achieving a fitness level of 87.71%. The resulting discrete-time transfer function is:

$$G(z) = \frac{0.0219}{z - 0.9173} \tag{1}$$

The identified velocity model was augmented with a discrete-time integrator, resulting in a second-order state-space representation. The system matrices are:

$$A = \begin{pmatrix} 0.9173 & 0 \\ 0.01 & 1 \end{pmatrix} \; B = \begin{pmatrix} 0.0219 \\ 0 \end{pmatrix}$$
$$C = \begin{pmatrix} 0 & 1 \end{pmatrix} \quad D = (0) \tag{2}$$

$x = \begin{pmatrix} v \\ p \end{pmatrix}$, where v represents the velocity and p the position; u is the PWM input command.

The equivalent transfer function is:

$$H(z) = \frac{0.0002191}{z^2 - 1.917\ z + 0.9173} \tag{3}$$

having the sampling period $T_s = 0.01 sec.$

Simulation results for this model are shown in Figure 3.

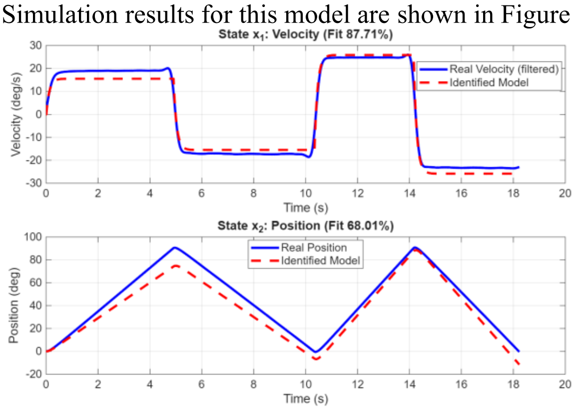

Fig. 3. Resulting model

IV. Control Design

A. PD Controller

A classical [21] PID controller, with transfer function (4), is designed as a baseline control strategy.

$$C(z) = K_p + \frac{K_i T_s}{z - 1} + \frac{K_d(z-1)}{(T_f + T_s)z - T_f} \tag{4}$$

The controller gains are tuned empirically to achieve a satisfactory compromise between rise time, overshoot, and steady-state error. As the model contains an integrator, a PD control was selected to maximize the transient response speed and ensure robust stability without introducing the phase lag associated with integration. The final design resulted in a PD controller with a proportional gain $K_p = 99.84$, a derivative gain $K_d = 5.06$, and a derivative filter time constant $T_f = 0.2\ seconds$. The test scenario utilized a multi-step reference trajectory designed to evaluate the system response across different operating points. The reference signal included step changes to $10, 20, 40$ and 60 degrees. The closed-loop response of the system is depicted in Figure 4. All simulations were conducted in Matlab. The quantitative analysis of the simulation yields a tracking Mean Absolute Error (MAE) of 4.05 and a Root Mean Square Error (RMSE) of 11.72. The linear, ramp-like convergence to the setpoint, rather than a standard exponential decay, is strictly dictated by the 100% PWM saturation limit of the physical actuator during large step changes.

B. LQG Control Design

Next, we consider an LQG controller [22], [23] designed based on model (2). Since only the position is measured, a discrete-time Kalman filter is designed to estimate the full state vector. Due to space constraints, the design steps are omitted; the reader is referred to [23].

For the Kalman filter, the process noise covariance matrix was selected as $Q = diag(2, 0.01)$. A significantly higher variance was assigned to the velocity to account for unmodeled dynamics. The measurement noise covariance was set to $R = 0.05$. This tuning resulted in a steady-state Kalman gain of $L = [4.65, 0.8]^T$, using a correction to the velocity estimate. For the real-time implementation, the gain was computed offline and kept constant to reduce computational complexity. The effectiveness of the Kalman filter was validated in simulation using experimental data, where the observer achieved a fitness score of 99.98% for the position and 91.63% for the velocity.

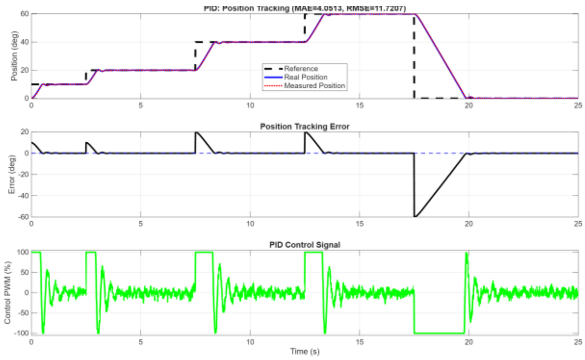

Fig. 4. Closed loop trajectories with PD Controller

For the LQR, the state weighting matrix $Q_{LQR} = diag(2,400)$ was chosen, to prioritize the minimization of position error. The control effort weighting was set to $R_{LQR} = 2$ to maintain the PWM signal as low as possible. The optimization yielded a constant feedback gain vector of $K = [1.53, 13.90]$. The control law incorporated the pre-calculated reference compensation factor $N_{fix} = 13.90$ to eliminate steady-state errors. The final discrete-time control law implemented on the embedded system is:

$$u[k] = N_{fix} r[k] - K\hat{x}[k] \tag{5}$$

where $u[k]$ represents the control input (PWM duty cycle) at sampling instant k, $r[k]$ denotes the desired reference position, and $\hat{x}[k]$ is vector estimated by the Kalman filter. It is important to note that tracking is achieved via a feedforward pre-compensation term N_{fix}, while the LQR state-feedback $K\hat{x}[k]$ provides closed-loop regulation around the nominal trajectory. Gaussian white noise was injected into both the process and the measurement to assess the robustness of the Kalman filter.

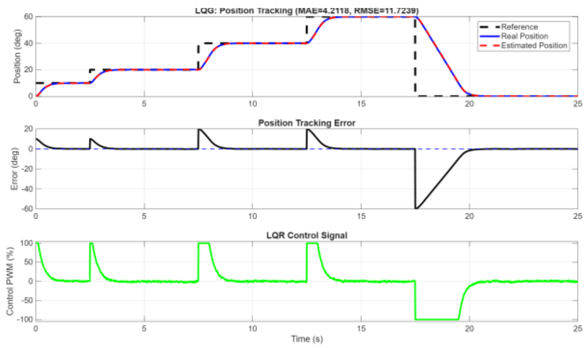

Fig. 5. Closed loop system trajectories using LQG controller

To validate the performance of the LQG architecture under realistic operating conditions, a closed-loop simulation was conducted. The same test scenarios was used as for the PD controller. The quantitative analysis of the simulation yields a tracking MAE of 4.21 and a RMSE of 11.72, almost the same as the PD controller. Furthermore, the Kalman filter demonstrated high precision, achieving a position estimation MAE of 0.06 despite the presence of measurement noise. The response of the closed-loop system, including position tracking, error evolution, and the estimated velocity profile, is illustrated in the Figure 5.

V. EXPERIMENTAL RESULTS

For the real-time physical experiments, the control algorithms were implemented on a Arduino Mega microcontroller, operating at a sampling period of 0.01 seconds. The PD and LQG were implemented and validated on the actuation unit of the WRIST-X rehabilitation robot. The experiments utilized the same multi-step reference trajectory as in simulations for both controllers to ensure a consistent performance assessment.

The experimental response of the system using the PD controller is presented in Figure 6. The PD controller achieves a MAE of 3.4 and a RMSE of 10.68. However, the aggressive tuning of the proportional term causes the PWM output to instantly saturate at 100% during step transitions. Consequently, the motor operates at its maximum varying velocity limit, resulting in a linear ramp-like position profile. This saturation phenomenon dominates the transient phase. Despite the physical limitations, the controller ensures stability and successfully eliminates steady-state error. The large discrepancy between the reference and the actual position during transitions is strictly a consequence of the maximum speed constraints of the DC motor under load, rather than a deficiency in the control itself. While this configuration offers a rapid response time, in rehabilitation contexts soft, compliant motions are prioritized over rigid positioning.

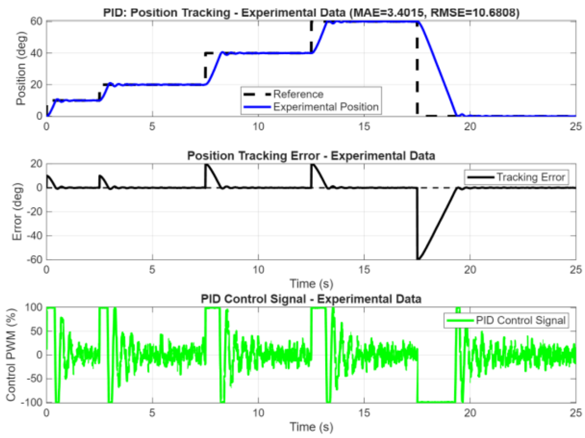

Fig. 6. Experimental result with PD

Following the baseline evaluation, the Linear Quadratic Gaussian (LQG) architecture was deployed under identical test conditions. The system's response is illustrated in Figure 7. The LQG framework yielded a higher MAE of 5.46 and an RMSE of 10.49 but provided a significant advantage regarding actuator usage.

The results confirm that the large amplitude of the reference forces the system into the saturation region, regardless of the control algorithm used. However, a distinct difference is observed in the actuator usage. In contrast to the aggressive PD response, the LQG control generates a significantly more tempered command that remains within the linear operating range of the driver, effectively avoiding the hard clamping at 100% duty cycle. Consequently, the transient phase is smoother, reducing mechanical stress. Furthermore, once the target position is achieved, the control signal settles into a stable holding torque. Unlike the derivative term in the PD which amplifies encoder quantization noise, the LQR feedback relies on the Kalman filter's smoothed state estimates. It is important to note that a minor steady-state error persists despite the application of the reference pre-compensation gain. This small deviation is attributed to unmodeled effects, primarily static friction in the joint transmission, which the linear state-feedback law cannot fully overcome when the error signal becomes small.

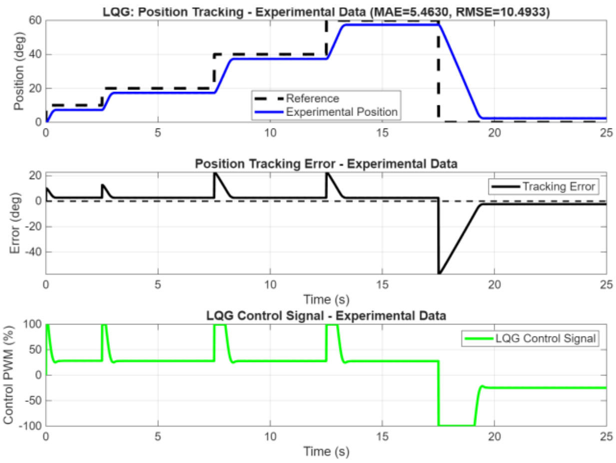

Fig. 7. Experimental result with LQG

VI. Conclusions

This paper presented a comparative study between two model-based control strategies applied to a DC motor actuating the joint of a rehabilitation robot. Starting from experimental data, a low-order discrete-time model was identified and subsequently augmented with an integrator to serve as the basis for the synthesis of both a PD and LQG controllers. Experimental validation demonstrated that while the PD controller achieved superior tracking accuracy, its aggressive transient response is less suited for therapeutic interaction compared to LQG. The LQG leveraged the Kalman filter to generate a significantly smoother and more compliant control signal, mitigating high-frequency quantization noise.

Future work will focus on addressing the observed steady-state errors in the LQG response by augmenting the state-space model with friction compensation mechanisms and extending this control framework to the remaining joints of the multi-degree-of-freedom robotic system. While the current baseline effectively manages the nominal operating range, future work will explore robust H_∞control strategies to explicitly handle parametric variations and external perturbations across wider operating conditions.

Acknowledgment

This research was supported by the project New frontiers in adaptive modular robotics for patient-centered medical rehabilitation–ASKLEPIOS, funded by European Union – NextGenerationEU and Romanian Government, under National Recovery and Resilience Plan for Romania, contract no. 760071/23.05.2023, code CF 121/15.11.2022, with Romanian Ministry of Research, Innovation and Digitalization, within Component 9, investment I8.

References

[1] C. Hwang, P. Li, C. Liu and C. Chen, "Design and analysis of a brushless DC motor for applications in robotics," *IET Electric Power Applications,* vol. 6, no. 7, pp. 385-389, 2012.

[2] I. Isa Ali and B. Muhammad Ahmad, "The DC Motor Advantages: Key Benefits and Improvements over AC Motors," *Global Journal of Research in Engineering & Computer Sciences,* vol. 04, no. 05, pp. 83-88, 2024.

[3] S.-H. Yen, P.-C. Tang, Y.-C. Lin and C.-Y. Lin, "A Sensorless and Low-Gain Brushless DC Motor Controller Using a Simplified Dynamic Force Compensator for Robot Arm Application," *Sensors,* vol. 19, no. 14, pp. 1-20, 2019.

[4] T. Messay, J. Mustefa and A. Eliyas, "Performance investigation of DC motor angular velocity using optimal and robust control method," *Acta technica Corviniensis – Bulletin of Engineering,* vol. 14, no. 1, pp. 147-150, 2021.

[5] G. Liu, "On velocity estimation using position measurements," *Proceedings of the American Control Conference,* vol. 2, no. 2, pp. 1115-1120, 2002.

[6] T. Arun K., Principles of System Identification: Theory and Practice, CRC Press, 2014.

[7] B. Wise and N. Ricker, "Identification of finite impulse response models by principal components regression: Frequency-response properties," *Process Control and Quality,* vol. 4, pp. 77-86, 1992.

[8] S. Das, "Modeling DC Motors and Their Control," in *Modeling for Hybrid and Electric Vehicles Using Simscape*, Cham, Springer International Publishing, 2021, pp. 47-71.

[9] X. Bian, Z. Wei, J. He, F. Yan and L. Liu, "A Two-Step Parameter Optimization Method for Low-Order Model-Based State-of-Charge Estimation," *IEEE Transactions on Transportation Electrification,* vol. 7, no. 2, pp. 399-409, 2021.

[10] V. Richard, Optimal Control, Birkhäuser Boston, MA, 2010.

[11] F. L. Lewis, D. L. Vrabie and V. L. Syrmos, Optimal Control, Hoboken, NJ: Wiley, 2012.

[12] J. Swevers, C. Ganseman, D. B. Tukel, J. De Schutter and H. Van Brussel, "Optimal robot excitation and identification," *IEEE T. on Robotics and Automation,* vol. 13, no. 1, pp. 53-65, 1997.

[13] J.J.E. Slotine and W. Li, Applied nonlinear control, Prentice Hall, 1991.

[14] D. Kostic, B. d. Jager, M. Steinbuch and R. Hensen, "Modeling and identification for high-performance robot control: an RRR-robotic arm case study," *IEEE Transactions on Control Systems Technology,* vol. 12, no. 6, pp. 904-919, 2004.

[15] J. Mehrholz, M. Pohl, T. Platz, J. Kugler and B. Elsner, "Electromechanical and robot-assisted arm training for improving activities of daily living, arm function, and arm muscle strength after stroke," *Cochrane Database of Systematic Reviews,* no. 9, 2018.

[16] W. Khalil and E. Dombre, Modeling, Identification and Control of Robot Manipulators, London: Hermes Penton Ltd, 2004.

[17] S.-D. Stiole, et al, "Design and Control of a New Wrist Rehabilitation Robot," in *Proceedings of ICINCO 2025*, Marbella, Spain, 2025.

[18] S.-D. Sim et al, "Online identification using Markov coefficients: application to a DC motor," in *29th International Conference on System Theory, Control and Computing (ICSTCC)*, Cluj-Napoca, Romania, 2025.

[19] K. Karel J., System Identification: An Introduction, Springer, 2011.

[20] L. Ljung, System Identification: Theory for the User, Upper Saddle River, NJ: Prentice Hall PTR, 1999.

[21] K. J. Åström and T. Hägglund, Advanced PID Control, Research Triangle Park, NC: ISA - The Instrumentation, Systems, and Automation Society, 2006.

[22] G. F. Franklin, J. D. Powell and M. L. Workman, Digital Control of Dynamic Systems, Menlo Park, CA: Addison-Wesley, 1998.

[23] B. D. O. Anderson and J. B. Moore, Optimal Control: Linear Quadratic Methods, Englewood Cliffs, NJ: Prentice Hall, 1990.